KERNFORSCHUNGSZENTRUM

KARLSRUHE

März 1965

KFK 253

Institut für Angewandte Reaktorphysik

The Balanced Oscillator Experiment

L. Caldarola

GESELLSCHAFT FÜR KERNFORSCHUNG M. B. H.

KARLSRUHE

The Balanced Oscillator Experiment*

Von L. CALDAROLA**

(Institut für Angewandte Reaktorphysik Kernforschungszentrum Karlsruhe)

With 12 figures in the text

(Received November 3, 1964)

Abstract. The "Balanced Oscillator Experiment" is a new type of oscillator experiment to measure transfer functions of nuclear fast reactors.

The technique consists in injecting in a reactor at the same time sinusoidal signals of reactivity and coolant flow of the same frequency and related each other in such a way that the coolant temperatures remain constant.

In addition to the Doppler reactivity coefficient, this new method allows to measure the fuel thermal conductivity and the heat transfer coefficient between fuel and coolant.

Numerical examples are included with reference to the Southwest Experimental Fast Oxide Reactor (Sefor). (Bibl. 3.)

1. Introduction

The "Balanced Oscillator Experiment" consists in injecting in a fast reactor at the same time sinusoidal signals of reactivity and coolant flow of the same frequency and related each other in such a way that the coolant temperatures remain constant.

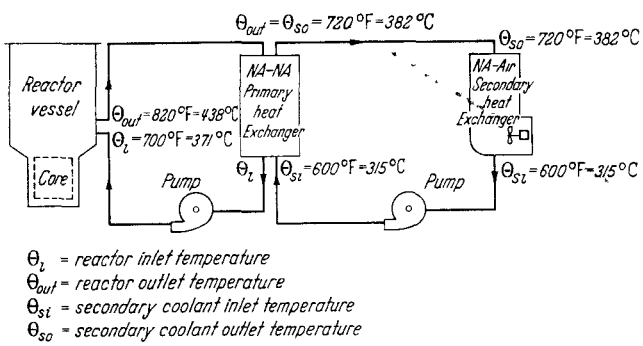

Fig. 1. Schematic reactor flow diagram (Sefor)

During the experiment the inlet coolant temperature must be kept constant by other means which are discussed later in para 6.

In this way the Doppler effect is the only reactivity temperature effect which is present during the experiment.

Fig. 1 shows the schematic reactor flow diagram.

Fig. 2 shows a schematic diagram of all the signals. The input signals to reactor are:

(i) reactivity signal $\Delta k = \Delta k_m \sin \omega t$, (1)

(ii) coolant flow signal $\Delta\mu = \Delta\mu_m \sin(\omega t + \alpha)$. (2)

The amplitude ratio, $\Delta\mu_m/\Delta k_m$, and the phase shift "α" of the two input signals must be chosen at any frequency in such a way that the outlet coolant temperature, Θ_{out}, remains constant. That is:

$$\Delta\Theta_{\text{out}} = 0. \tag{3}$$

The outlet coolant temperature is measured by a thermocouple (Fig. 2). $\Delta\mu_m/\Delta k_m$ and "α" are obviously function of "ω".

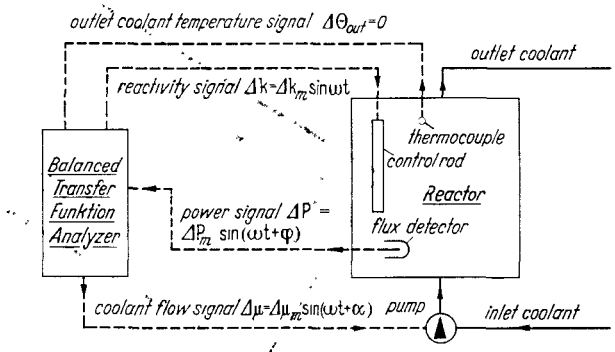

Fig. 2. Balanced oscillator experiment — Schematic Diagram of the signals

The power signal ΔP is measured by means of a flux detector (Fig. 2). The "Balanced Transfer Function Analyser" (Fig. 2) allows us to evaluate the two transfer functions

$$\frac{\Delta\mu^*(j\omega)/\mu_0}{\Delta P^*(j\omega)/P_0} \tag{4}$$

and

$$\frac{\Delta P^*(j\omega)/P_0}{\Delta k^*(j\omega)/\beta} \tag{5}$$

where

"*" indicates Laplace transform

subscript "$_0$" indicates steady state condition

β = fraction of delayed neutrons.

2. Physical Fundamentals

In this paragraph we intend to find out which conditions should the amplitude ratio $\Delta\mu_m/\Delta k_m$ and the phase shift "α" satisfy in order to keep the coolant temperatures constant.

* This paper has been prepared within the framework of the association Euratom-Gesellschaft für Kernforschung mbH. in the field of fast breeder development.

** Euratom, Brussels, delegated to the Karlsruhe Fast Reactor Project Institut für Angewandte Reaktorphysik.

The reactor can be considered as divided in "n" cooling channels each including a fuel rod and its associated coolant. The heat balance equation of the coolant in an average channel is the following:

$$\frac{2\pi Rh}{c}\,\frac{T_s-\Theta}{\mu/n}=\frac{\partial\Theta}{\partial z}+\frac{1}{v}\,\frac{\partial\Theta}{\partial t} \tag{1}$$

where

h = heat transfer coeff. between fuel surface and coolant (including the cladding)
R = radius of fuel rod
c = specific heat capacity of the coolant
T_s = fuel surface temperature
Θ = coolant temperature
z = axial coordinate
v = coolant speed
t = time
n = number of cooling channels.

Eq. (1) can give $\partial\Theta/\partial t=0$ only if:

$$\frac{T_s-\Theta}{\mu}=\frac{T_{s0}-\Theta_0}{\mu_0}=\text{function of "}z\text{" only} \tag{2}$$

where subscript "$_0$" indicates initial steady state conditions. Taking into account (2), eq. (1) becomes:

$$\frac{2\pi Rh}{c}\,\frac{T_{s0}-\Theta_0}{\mu_0/n}=\frac{\partial\Theta}{\partial z}+\frac{1}{v}\,\frac{\partial\Theta}{\partial t}\,. \tag{3}$$

If we introduce the change of coolant temperature, $\Delta\Theta$

$$\Delta\Theta=\Theta-\Theta_0 \tag{4}$$

eq. (3) becomes:

$$\frac{2\pi Rh}{c}\,\frac{T_{s0}-\Theta_0}{\mu_0/n}=\frac{d\Theta_0}{dz}+\frac{\partial\Delta\Theta}{\partial z}+\frac{1}{v}\,\frac{\partial\Delta\Theta}{\partial t}\,. \tag{5}$$

It is:

$$\frac{2\pi Rh}{c}\,\frac{T_{s0}-\Theta_0}{\mu_0/n}=\frac{d\Theta_0}{dz}\,. \tag{6}$$

Eq. (5) becomes therefore:

$$\frac{\partial\Delta\Theta}{\partial z}+\frac{1}{v}\,\frac{\partial\Delta\Theta}{\partial t}=0. \tag{7}$$

Eq. (7) associated to the boundary condition that the inlet coolant temperature, Θ_i, is constant ($\Delta\Theta_i=0$), gives:

$$\Delta\Theta=0. \tag{8}$$

We have therefore shown that condition (2) is necessary and sufficient in order to keep the coolant temperatures constant with time.

Taking into account (4) and (8), condition (2) may be written as follows:

$$\frac{\mu}{\mu_0}=\frac{T_s-\Theta}{T_{s0}-\Theta_0}=\frac{T_s-\Theta_0}{T_{s0}-\Theta_0}\,. \tag{9}$$

Introducing

$$\Delta\mu=\mu-\mu_0 \tag{10}$$

and

$$\Delta T_s=T_s-T_{s0} \tag{11}$$

eq. (9) becomes:

$$\frac{\Delta\mu}{\mu_0}=\frac{\Delta T_s}{T_{s0}-\Theta_0}\,. \tag{12}$$

The Laplace transform of eq. (12) is:

$$\frac{\Delta\mu^*}{\mu_0}=\frac{\Delta T_s^*}{T_{s0}-\Theta_0}\,. \tag{13}$$

It is:

$$T_{s0}-\Theta_0=\frac{R}{2h}\,\frac{P_0}{V_f}\,M(z) \tag{14}$$

where:

P_0 = reactor power at steady state
V_f = volume of fuel in reactor $=n\pi R^2H$ (H being the height of the fuel rod)
$M(z)$ = normalized function expressing power distribution along the axis of a fuel rod $\left[\frac{1}{H}\int_0^H M(z)\,dz=1\right]$.

Since the coolant temperatures are constant, it is [according to Ref. 2, para 2, eq. (20)]:

$$\Delta T_s^*=\frac{R}{2h}\,\frac{1}{V_f}\,F_s(s\cdot t_r)\,M(z)\,\Delta P^*(s) \tag{15}$$

where

$\Delta P^*(s)$ = Laplace transform of the power change

and

$F_s(s\cdot t_r)$ = normalized transfer function between fuel surface temperature and power $[F_s(0)=1]$

t_r = radial time scale $=\frac{\varrho_f c_f}{\lambda}R^2=$

$=\frac{\text{fuel density}\cdot\text{fuel specific heat capacity}}{\text{fuel thermal conductivity}}\times$

$\times(\text{radius})^2$.

Putting (14) and (15) in (13), we have:

$$\frac{\Delta\mu^*}{\mu_0}=\frac{\Delta T_s^*}{T_{s0}-\Theta_0}=F_s(s\cdot t_r)\,\frac{\Delta P^*}{P_0} \tag{16}$$

which is independent on the axial coordinate "z".

In the time domain eq. (16) becomes:

$$\frac{\Delta\mu}{\mu_0}=\frac{\Delta T_s}{T_{s0}-\Theta_0}=\frac{1}{P_0}\int_0^t f_s(x)\,\Delta P(t-x)\,dx \tag{17}$$

where

$$f_s(t)=L^{-1}[F_s(s\cdot t_r)] \tag{18}$$

and L^{-1} indicates antitransformation.

The demonstration given in this paragraph starts from the assumption (2) where μ can be dependent on "z" which is physically impossible. At the end [eqs. (16) and (17)] we find out that μ is function only of the time.

In Appendix 1 a more refined demonstration is given: starting from condition (17) where μ is only a time dependent function, it is shown that the coolant temperatures remain constant.

Eq. (16) allows us to find which conditions should the amplitude ratio $\Delta\mu_m/\Delta k_m$ and the phase shift "α" satisfy, in order to keep the coolant temperatures constant.

It is:

$$\left.\begin{aligned}D(j\omega)&=\frac{\Delta P^*(j\omega)/P_0}{\Delta k^*(j\omega)/\beta}\\&=\text{reactor power transfer function.}\end{aligned}\right\} \tag{19}$$

Taking into account (16) and (19) we have:

$$\frac{\Delta\mu^*(j\omega)}{\Delta k^*(j\omega)}=\frac{\Delta\mu^*(j\omega)}{\Delta P^*(j\omega)}\cdot\frac{\Delta P^*(j\omega)}{\Delta k^*(j\omega)}=\frac{\mu_0}{\beta}\,D(j\omega)\,F_s(j\omega t_r) \tag{20}$$

and therefore:

$$\frac{\Delta\mu_m}{\Delta k_m} = \frac{\mu_0}{\beta}\,|D(j\omega)|\cdot|F_s(j\omega t_r)| \tag{21}$$

$$\alpha = \varphi_D(j\omega) + \varphi_s(j\omega t_r). \tag{22}$$

φ_D and φ_s being the phases respectively of the functions $D(j\omega)$ and $F_s(j\omega t_r)$.

3. Results obtainable from the new oscillator experiment

We have already said in para 1 that the "Balanced Transfer Function Analyser" allows us to evaluate

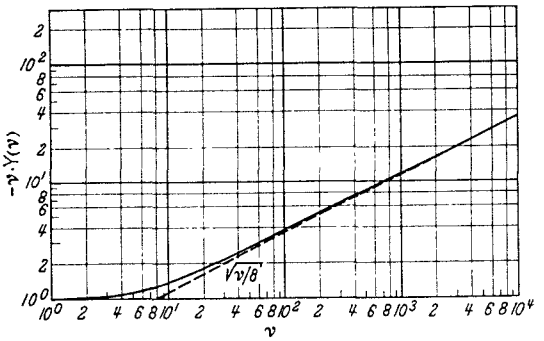

Fig. 3. Diagram of the function $-\nu\,Y(\nu)$

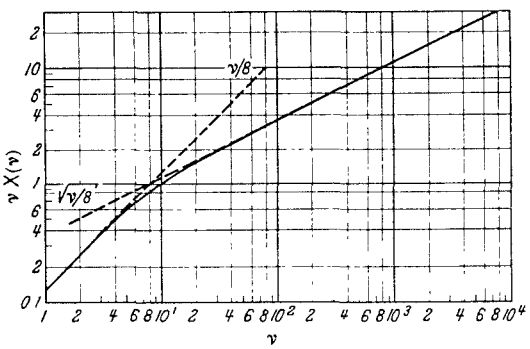

Fig. 4. Diagram of the function $\nu X(\nu)$

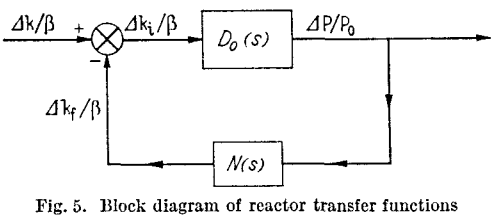

Fig. 5. Block diagram of reactor transfer functions

the two following transfer functions:

$$F_s(j\omega t_r) = \frac{\Delta\mu^*(j\omega)/\mu_0}{\Delta P^*(j\omega)/P_0} \tag{1}$$

and

$$D(j\omega) = \frac{\Delta P^*(j\omega)/P_0}{\Delta k^*(j\omega)/\beta}. \tag{2}$$

As we have already shown in para 2 [eq. (16)], $F_s(j\omega t_r)$ is the transfer function between fuel surface temperature and power.

3.1. Determination of the parameters t_r and γ from the transfer function $F_s(j\omega t_r) = \frac{\Delta\mu^*(j\omega)/\mu_0}{\Delta P^*(j\omega)/P_0}$

The author has found the following theoretical expression for $F_s(\sigma)$ with $\sigma = s t_r$ (Ref. 2):

$$F_s(\sigma) = \frac{1/\sigma Z(\sigma)}{1+\gamma/Z(\sigma)} \tag{3}$$

where

$$\left.\begin{aligned} t_r &= \text{radial time scale} = \frac{\varrho_f c_f}{\lambda} R^2 = \\ &= \frac{\text{fuel density} \times \text{fuel specific heat capacity}}{\text{fuel thermal conductivity}} \times \\ &\times (\text{radius})^2, \end{aligned}\right\} \tag{4}$$

$$\left.\begin{aligned} \gamma &= \frac{\lambda}{2hR} = \\ &= \frac{\text{fuel thermal conductivity}}{2 \times \text{heat transfer coefficient} \times \text{radius}}, \end{aligned}\right\} \tag{4'}$$

$$Z(\sigma) = -\frac{J_0(\sqrt{-\sigma})}{2\sqrt{-\sigma}\,J_1(\sqrt{-\sigma})}. \tag{5}$$

J_0 and J_1 being Bessel functions of the first kind.

Putting $\sigma = jv = j\omega t_r$, we can write:

$$Z(jv) = X(v) + j\,Y(v). \tag{6}$$

With $X(v)$ and $Y(v)$ respectively real and imaginary part of $Z(jv)$. Introducing (6) in (3), we can write:

$$\frac{1}{F_s(jv)} = -v\,Y(v) + j[vX(v) + \gamma t_r \omega]. \tag{7}$$

$F_s(j\omega t_r)$ is also determined experimentally by means of eq. (1). Indicating with $M_s(\omega t_r)$ and $\varphi_s(\omega t_r)$ respectively modulus and phase of $F_s(j\omega t_r)$, we have:

$$\frac{1}{F_s(j\omega t_r)} = \frac{\cos\varphi_s}{M_s} - j\frac{\sin\varphi_s}{M_s}. \tag{8}$$

By comparing (7) with (8) we have:

$$\frac{\cos\varphi_s}{M_s} = -v\,Y(v) \tag{9}$$

and

$$-\frac{\sin\varphi_s}{M_s} = vX(v) + \gamma t_r\,\omega. \tag{10}$$

The functions $-v\,Y(v)$ and $vX(v)$ have been calculated and are given respectively in Figs. 2 and 4.

For a chosen value of ω we can evaluate $\cos\varphi_s/M_s$ experimentally. Using eq. (9), and Fig. 3 we get v and, since $v = \omega t_r$, t_r in determined.

In eq. (10) the term $-\sin\varphi_s/M_s$ on the left side is evaluated experimentally for the chosen ω. $vX(v)$ is also known because v is known, and we can therefore determine $\gamma \cdot t_r$.

The functions $-v\,Y(v)$ and $vX(v)$ have been programmed on the IBM 7070 computer, so that t_r and γ can be more precisely determined by means of numerical methods instead of using the graphs of Figs. 3 and 4. From t_r and γ, it is possible to evaluate the thermal conductivity, λ, and the heat transfer coefficient, h, if the density, ϱ, the specific heat capacity, c, and radius, R, of the fuel rod have been previously determined.

3.2. Determination of the Doppler power coefficient and of the parameter σ_1/t_r from the reactor transfer function,

$$D(j\omega) = \frac{\Delta P^*(j\omega)/P_0}{\Delta k^*(j\omega)/\beta}.$$

Fig. 5 shows a schematic block diagram of the reactor transfer functions defined as:

$$D_0(s) = \frac{\Delta P^*(s)/P_0}{\Delta k_i^*(s)/\beta} = \text{zero power transfer function}, \tag{11}$$

$$N(s)=\frac{\Delta k_f^*(s)/\beta}{\Delta P^*(s)/P_0}=\text{feedback transfer function}, \quad (12)$$

$$\left.\begin{aligned} D(s)&=\frac{\Delta P^*(s)/P_0}{\Delta k^*(s)/\beta}=\frac{D_0(s)}{1+D_0(s)\cdot N(s)}\\ &=\text{power transfer function}\end{aligned}\right\} \quad (13)$$

where:

$$\Delta k=\Delta k_i+\Delta k_f. \quad (14)$$

Since the coolant temperatures are constant, the reactivity feedback (Δk_f) will depend only on the fuel temperatures. It is:

$$\Delta k_f=\gamma_f \Delta T_{\text{eff}} \quad (15)$$

where:

γ_f = fuel temperature coefficient (mainly Doppler)
T_{eff} = effective fuel temperature.

The effective fuel temperature is defined by:

$$\Delta T_{\text{eff}}=\frac{\int_{\text{all rods}} \Phi\Phi' \Delta T_{\text{av}}\, dV}{\int_{\text{all rods}} \Phi\Phi' dV}. \quad (16)$$

Φ and Φ' being respectively flux and adjoint flux, V volume and T_{av} the average temperature of a section of a fuel rod. Since the coolant temperatures are constant, ΔT_{av} will depend only on ΔP. It is [according to Ref. 2 para 2 eq. (22)]:

$$\Delta T_{\text{av}}^*=\frac{R}{2h}\left(1+\frac{1}{8\gamma}\right)F_{\text{av}}(s\cdot t_r)\frac{M(z)}{V_f}\Delta P^*(s) \quad (17)$$

where:

$F_{\text{av}}(st_r)$ = normalized transfer function between average fuel temperature and power $[F_{\text{av}}(0)=1]$.

Putting (16) and (17) in (15), and taking into account that $V_f=n\pi R^2 H$, we get:

$$\Delta k_f^*=G\cdot F_{\text{av}}(s\cdot t_r)\frac{1}{nH}\Delta P^*(s) \quad (18)$$

where:

$$\left.\begin{aligned} G&=\text{Doppler power coefficient}\\ &=\gamma_f A_f \frac{1}{2\pi Rh}\left(1+\frac{1}{8\gamma}\right),\end{aligned}\right\} \quad (19)$$

$$A_f=\frac{\int_{\text{all rods}} \Phi\Phi' M(z)\, dV}{\int_{\text{all rods}} \Phi\Phi' dV}. \quad (20)$$

Taking into account (18), eq. (12) becomes:

$$N(s)=\frac{P_0}{nH}\cdot\frac{1}{\beta}G\cdot F_{\text{av}}(s\cdot t_r). \quad (21)$$

The author has shown in Ref. 2 that the function $F_{\text{av}}(s\cdot t_r)$ with very good approximation is given by:

$$F_{\text{av}}(s\cdot t_r)\cong\frac{1}{1+st_r/\sigma_1}. \quad (22)$$

$-\sigma_1$ being the first root of the Bessel functions equation:

$$\frac{J_0(\sqrt{-\sigma})}{2\sqrt{-\sigma}\,J_1(\sqrt{-\sigma})}=\gamma. \quad (23)$$

Putting (22) in (21), we get:

$$N(s)\cong\frac{P_0}{nH}\frac{1}{\beta}G\frac{1}{1+st_r/\sigma_1}. \quad (24)$$

From eq. (13) we have

$$N(s)=\frac{1}{D(s)}-\frac{1}{D_0(s)}. \quad (25)$$

From (24) and (25) we obtain (putting $s=j\omega$):

$$\frac{P_0}{nH}\frac{G}{\beta}\frac{1}{1+j\omega t_r/\sigma_1}=\frac{1}{D(j\omega)}-\frac{1}{D_0(j\omega)}. \quad (26)$$

If φ_D and φ_{D_0} are the phases respectively of $D(j\omega)$ and $D_0(j\omega)$, from (26) we have:

$$\left.\begin{aligned} \frac{P_0}{nH}\frac{G}{\beta}&=\frac{1}{|D|\cos\varphi_D}\times\\ &\times\frac{1+\left|\frac{D}{D_0}\right|^2-2\left|\frac{D}{D_0}\right|\cos(\varphi_D-\varphi_{D_0})}{1-\left|\frac{D}{D_0}\right|\frac{\cos\varphi_{D_0}}{\cos\varphi_D}}\end{aligned}\right\} \quad (27)$$

and

$$\frac{\sigma_1}{t_r}=\omega\operatorname{ctg}\varphi_D\cdot\frac{1-\left|\frac{D}{D_0}\right|\frac{\cos\varphi_{D_0}}{\cos\varphi_D}}{1-\left|\frac{D}{D_0}\right|\frac{\sin\varphi_{D_0}}{\sin\varphi_D}}. \quad (28)$$

It is:

$$\lim_{\omega\to 0}\left|\frac{D}{D_0}\right|=0, \quad (29)$$

$$\lim_{\omega\to 0}\cos\varphi_{D_0}=0, \quad (30)$$

$$\lim_{\omega\to 0}\cos\varphi_D=1. \quad (31)$$

Taking into account (29); (30) and (31), eq. (27) becomes:

$$\lim_{\omega\to 0}\frac{1}{|D|}=\frac{P_0}{nH}\frac{G}{\beta}. \quad (32)$$

For ω very small (in Sefor smaller than $3\cdot 10^{-3}\,\text{sec}^{-1}$), the power transfer function $D(j\omega)$ tends to the asymptotic value $nH\beta/PG$. Since P_0/nH and β are known, eq. (32) allows to determine the Doppler power coefficient G. We can conclude that G can be determined by measuring the transfer function $D(j\omega)$ only.

Eq. (28) allows to determine the parameter, σ_1/t_r. From the point of view of the accuracy, it is convenient to carry out this evaluation when $\operatorname{ctg}\varphi_D\cong 1$ that is when $\omega\cong\sigma_1/t_r$.

The determination of σ_1/t_r implies in the most general cases the measurement of both the transfer functions $D(j\omega)$ and $D_0(j\omega)$. In some cases the conditions (29) and (30) are already satisfied in the frequency region under consideration and σ_1/t_r is than more simply given by

$$\frac{\sigma_1}{t_r}=\omega\operatorname{cotg}\varphi_D. \quad (33)$$

This happens when:

$$\frac{\sigma_1}{t_r}\ll\lambda_\infty \quad (34)$$

where

$$\lambda_\infty=\frac{1}{\sum_{i=1}^{i=6}\beta_i}, \quad (35)$$

β_i and λ_i being respectively fraction and decay constant associated to the "i" th group of delayed neutrons. The determination of σ_1/t_r can be used as a countercheck of the results obtained in para 3.1. Since t_r and γ have already been determined (para 3.1) and σ_1 is function of γ (Fig. 6), the ratio σ_1/t_r can be also theoretically calculated and compared with that obtained experimentally.

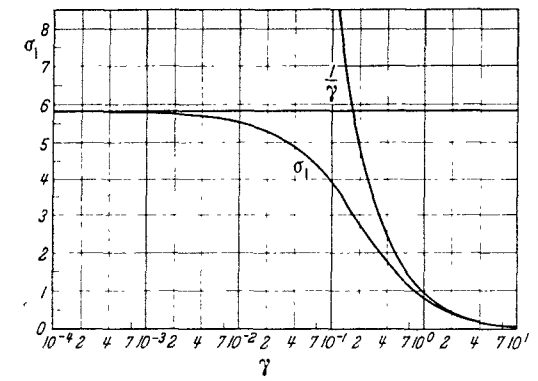

Fig. 6. First root $-\sigma_1$ of the equation $\frac{J_0(j\sqrt{-\sigma})}{2\sqrt{-\sigma}J_1(j\sqrt{-\sigma})} = \gamma$ as function of γ

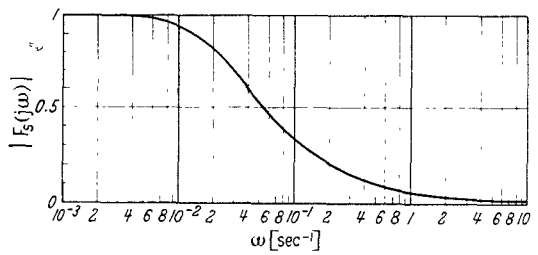

Fig. 7. Frequency response of the transfer function $F_s(j\omega)$—Amplitude diagram (Sefor)

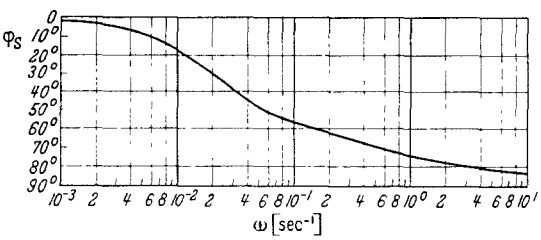

Fig. 8. Frequency response of the transfer function $F_s(j\omega)$ — Phase diagram (Sefor)

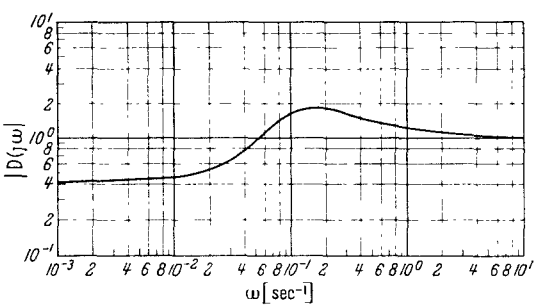

Fig. 9. Frequency response of the reactor power transfer function $D(j\omega)$—Amplitude diagram (Sefor)

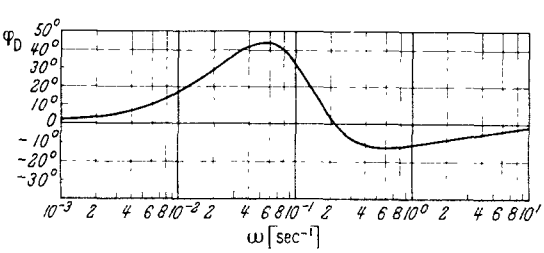

Fig. 10. Frequency response of the reactor power transfer function $D(j\omega)$—Phase diagram (Sefor)

4. Numerical examples for Sefor reactor

Figs. 7 and 8 show respectively amplitude (M_s) and phase (φ_s) of the function $F_s(j\omega)$ as it is expected to be in Sefor.

Taking for example $\omega = 0.0625$ rad/sec, we have:

$$M_s = 0.4537 \quad \text{from Fig. 7,} \tag{1}$$

$$\varphi_s = -51°5 \quad \text{from Fig. 8.} \tag{2}$$

From (1) and (2), we have:

$$\frac{\cos\varphi_s}{M_s} = \frac{0.6225}{0.4537} = 1.375 = -\nu Y(\nu), \tag{3}$$

$$-\frac{\sin\varphi_s}{M_s} = \frac{0.7826}{0.4537} = 1.73 = \nu X(\nu) + \gamma t_r \omega. \tag{4}$$

From Fig. 3, we see that:

$$-\nu Y(\nu) = 1.375 \text{ when } \nu = 10. \tag{5}$$

We can therefore determine t_r:

$$t_r = \frac{\nu}{\omega} = \frac{10}{0.0625} = 160 \text{ secs.} \tag{6}$$

From Fig. 4, when $\nu = 10$, we have

$$\nu X(\nu) \cong 1.03. \tag{7}$$

From eq. (4) we get:

$$\gamma t_r = \frac{1.73 - 1.03}{0.0625} = 11.2 \text{ secs} \tag{8}$$

and therefore we determine γ

$$\gamma = \frac{11.2}{160} = 0.07. \tag{9}$$

From Fig. 6 for $\gamma = 0.07$ we get:

$$\sigma_1 = 4.4068 \tag{10}$$

and

$$\frac{\sigma_1}{t_r} = \frac{4.4068}{160} = 0.0276 \text{ rad/sec.} \tag{11}$$

Figs. 9 and 10 show respectively amplitude and phase of the power transfer function $D(j\omega)$ in the low frequency region as it is expected to be in the case of Sefor.

For $\omega < 3 \cdot 10^{-3}$ sec^{-1}, $|D(j\omega)|$ tends to the asymptotic value of 0.424 \$$^{-1}$. From eq. (28) of para 3.2 putting $\omega = 0$, we get

$$\frac{P_0}{nH}\frac{G}{\beta} = \frac{1}{0.424} = 2.36 \text{ \$}. \tag{12}$$

Since:

$$P_0 = 20 \text{ MW}, \tag{13}$$

$$nH = 500 \text{ m}, \tag{14}$$

$$\beta = 3.395 \cdot 10^{-3}. \tag{15}$$

G can be determined

$$G = \frac{2.36 \cdot 500 \cdot 3.395 \cdot 10^{-3}}{20} \cong 0.2\, \Delta k \cdot m/\text{MW}. \tag{16}$$

For $\omega = 0.029$ sec^{-1} (which is not too different from the theoretical value of σ_1/t_r given by 11), we have:

$$|D_0| = 4.24 \quad \text{(from Fig. 11),} \tag{17}$$

$$|D| = 0.622 \quad \text{(from Fig. 9),} \tag{18}$$

$$\varphi_{D_0} = -55° \quad \text{(from Fig. 12),} \tag{19}$$

$$\varphi_D = +36°8 \quad \text{(from Fig. 10).} \tag{20}$$

Using eq. (28) of para 3.2, we have:

$$\left.\begin{aligned}\frac{\sigma_1}{t_r} &= 0.029 \cdot 1.33 \frac{1-\frac{0.622}{4.24}\frac{0.82}{0.8}}{1+\frac{0.622}{4.24}\frac{0.57}{0.598}} \\ &= 0.029 \cdot 1.33 \cdot 0.740 = 0.0286\ (\mathrm{sec}^{-1}).\end{aligned}\right\} \quad (21)$$

The value of σ_1/t_r calculated by (21) differs slightly from that given by (11) because the reactivity feedback transfer function is only approximately expressed by one pole [eqs. (22) and (24) of para 3.2].

5. Comparison with the traditional oscillator experiment

With the traditional oscillator experiment only the reactivity signal is introduced in the reactor. The advantages of the "balanced oscillator experiment" in comparison with the traditional one, are mainly the following:

(i) Since the coolant temperatures are constant, it is possible to separate the Doppler temperature effect on reactivity from the other temperature effects. It is a real clean oscillator experiment.

(ii) The normalized transfer function $F_s(j\omega t_r)$ between fuel surface temperature and power is determined by indirect measurements. The direct measurement of $F_s(j\omega t_r)$ would imply the measurement of the fuel surface temperature, which is technically difficult and inaccurate. The measurement of $F_s(j\omega t_r)$ allows to determine the parameters γ and t_r and therefore the fuel conductivity, λ, and the heat transfer coefficient, h, can be calculated.

(iii) The normalized transfer function $F_{av}(j\omega t_r)$ between average fuel temperature and power is determined and therefore the parameter σ_1/t_r can be calculated.

With the traditional type of oscillator experiment the transfer function $F_s(j\omega)$ cannot be determined and therefore γ and t_r cannot be evaluated.

In addition, since the coolant temperatures are not kept constant, the Doppler temperature effect on reactivity is not rigorously separated from the other temperature effects. The calculation of the Doppler power coefficient, G, and of the parameter, σ_1/t_r, from the power transfer function $D(j\omega)$ is therefore more complicated and it is dependent upon the knowledge of the other reactivity coefficients and their associated time constants.

6. Final Comments

The method of introducing in a system two or more sinusoidal signals related in such a way that a specific physical quantity easily measurable does not change, can be considered a very general method to measure transfer functions indirectly. This "balance technique" may have a wide application especially when it is difficult to carry out the direct measurement of a transfer function.

A simple and well known example of "balance technique" is the Wheatstone Bridge to measure electric impedences. In the Wheatstone Bridge the impedences are balanced in modulus and phase in such a way that no current passes through the diagonal. When this condition is fulfilled, the unknown impedence can be determined by a simple relationship with the other three known impedences.

To end our comments about the application of the "balanced oscillator experiment" on Sefor, we must say that the coolant flow signal may cause a noticeable disturbance in the inlet coolant temperature, Θ_i, through the primary heat exchanger. Since Θ_i must be kept constant during the experiment, it is necessary to balance this effect. This may be obtained by introducing in the system a third signal $\Delta\xi = \Delta\xi_m \sin(\omega t + \delta)$ to the pump of the secondary coolant circuit (Fig. 1). $\Delta\xi_m$ and δ must of course chosen in such a way that no change occurs in Θ_i.

A better solution could be obtained by putting a by-pass value across the primary heat exchanger from

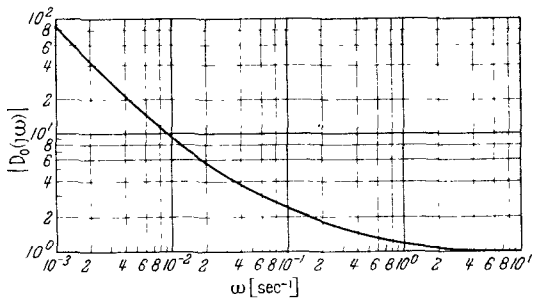

Fig. 11. Frequency response of the zero power transfer function $D_0(j\omega)$ — Amplitude diagram (Sefor)

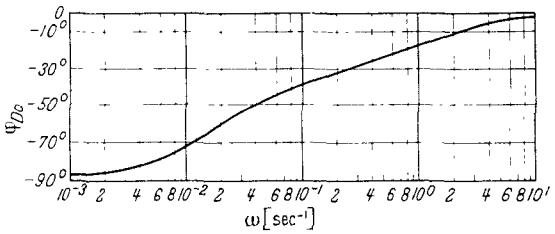

Fig. 12. Frequency response of the zero power transfer function $D_0(j\omega)$ — Phase diagram (Sefor)

the side of the primary coolant circuit (Fig. 1). This valve should of course be operated in such a way that Θ_i remains constant during the experiment.

In the analysis developed in this paper, the thermal capacity of the fuel cladding has been purposely neglected in order to show the essential parts of the new experiment. In the heat transfer coefficient "h" are included the heat transfer coefficients fuel to cladding, internal to external surface of the cladding and cladding to coolant. However, if the thermal capacity of the fuel cladding must be taken into account, the philosophy of the experiment is still valid, but the mathematical relationships will be slightly more complicated.

Appendix I

Demonstration that the coolant temperatures, Θ. remain constant during the experiment $[\Delta\Theta(z;t) = 0]$

The heat balance equation of the coolant in a cooling channel is the following:

$$\frac{2\pi R h}{c}\,\frac{T_s - \Theta}{\mu/n} = \frac{\partial\Theta}{\partial z} + \frac{1}{v}\,\frac{\partial\Theta}{\partial t} \quad (1)$$

where:

R = radius of fuel rod
h = heat transfer coefficient between fuel and coolant (including the cladding)
c = specific heat capacity of the coolant
μ = coolant flow
T_s = surface fuel temperature
z = axial coordinate
v = coolant speed
t = time
n = number of cooling channels.

We introduce:

$$T_s = T_{s0} + \Delta T_s, \tag{2}$$

$$\Theta = \Theta_0 + \Delta\Theta, \tag{3}$$

$$\mu = \mu_0 + \Delta\mu \tag{4}$$

where subscript "$_0$" indicates initial steady state conditions and "Δ" variation from steady state condition.

The fuel surface temperature, T_s, may be expressed as function of the coolant temperature, Θ, and of the power, P [according to Ref. 2 para 2 eq. (20)]:

$$\left.\begin{aligned}\Delta T_s^*(st_r; z) = G_s(st_r)\,\Delta\Theta^*(s; z) + \\ + \frac{R}{2h} F_s(st_r) \frac{\Delta P^*(s)}{V_f} M(z)\end{aligned}\right\} \tag{5}$$

where:

"*" indicates Laplace transform
s = complex variable of Laplace transformation
V_f = volume of fuel in reactor $= n\pi R^2 H$ (H being the height of the fuel rod)
$M(z)$ = normalized function expressing power distribution along the axis of a fuel rod $\left[\frac{1}{H}\int_0^H M(z)\,dz = 1\right]$
t_r = radial time scale $= \frac{\varrho_f c_f}{\lambda} R^2 =$
$= \frac{\text{fuel density} \times \text{specific heat capacity}}{\text{fuel thermal conductivity}} \times$
$\times$ (radius)^2
$G_s(st_r)$ = normalized transfer function given in Ref. 2 para 2 eq. (23) [$G_s(0) = 1$]
$F_s(st_r)$ = normalized transfer function given in Ref. 2 para 2 eq. (24) [$F_s(0) = 1$].

It is [Ref. 2 para 2 eq. (24)]:

$$G_s(st_r) = 1 - \gamma t_r s F_s(st_r) \tag{6}$$

where:

$$\gamma = \frac{\lambda}{2hR} = \frac{\text{fuel thermal conductivity}}{2 \times \text{heat transfer coefficient} \times \text{Radius}}. \tag{7}$$

Eq. (5) becomes:

$$\left.\begin{aligned}\Delta T_s^*(st_r; z) = \Delta\Theta^*(s; z)[1 - \gamma t_r s F_s(st_r)] + \\ + \frac{R}{2h} F_s(st_r) \frac{M(z)}{V_f} \Delta P^*(s).\end{aligned}\right\} \tag{8}$$

Antitransforming to the time domain, (8) gives:

$$\left.\begin{aligned}\Delta T_s = \Delta\Theta - \gamma t_r \int_0^t \frac{df_s(x)}{dx} \Delta\Theta(z; t-x)\,dx + \\ + \frac{R \cdot M(z)}{2h V_f} \int_0^t f_s(x)\,\Delta P(t-x)\,dx\end{aligned}\right\} \tag{9}$$

where:

$$f_s(t) = L^{-1}[F_s(st_r)] \tag{10}$$

and L^{-1} indicates antitransformation.

We shall also remember that, at steady state conditions, it is:

$$\frac{2\pi Rh(T_{s0} - \Theta_0)}{c\mu_0/n} = \frac{\pi R^2 P_0}{c\mu_0 V_f/n} M(z) = \frac{d\Theta_0}{dz}. \tag{11}$$

Taking into account (2); (3); (4) and (9), eq. (1) becomes:

$$\left.\begin{aligned}\pi R^2 \frac{P_0 M(z)}{c\mu_0 V_f/n} \frac{1 + \frac{1}{P_0}\int_0^t f_s(x)\,\Delta P(t-x)\,dx}{1 + \frac{\Delta\mu}{\mu_0}} \\ = \frac{d\Theta_0}{dz} + \frac{\partial\Delta\Theta}{\partial z} + \frac{1}{v}\frac{\partial\Delta\Theta}{\partial t} + \\ + \frac{2\pi Rh\gamma t_r}{c\mu/n} \int_0^t \frac{df_s(x)}{dx} \Delta\Theta(z; t-x)\,dx.\end{aligned}\right\} \tag{12}$$

We must demonstrate that the condition

$$\frac{\Delta\mu}{\mu_0} = \frac{1}{P_0}\int_0^t f_s(x)\,\Delta P(t-x)\,dx \tag{13}$$

is necessary and sufficient to give $\Delta\Theta(z; t) = 0$.

Eq. (13) is equal to condition (17) of para 2.

In the Laplace domain eq. (13) is equivalent to:

$$\frac{\Delta\mu^*(s)}{\mu_0} = F_s(st_r)\frac{\Delta P^*(s)}{P_0} \tag{14}$$

which is equal to condition (16) of para 2.

Condition (13) is necessary because eq. (12) can give $\Delta\Theta = 0$ only if (13) is satisfied.

Taking into account (11) and (13), eq. (12) becomes:

$$\left.\begin{aligned}\frac{\partial\Delta\Theta}{\partial z} + \frac{1}{v}\frac{\partial\Delta\Theta}{\partial t} + \\ + \frac{2\pi Rh\gamma t_r}{c\mu/n} \int_0^t \frac{df_s(x)}{dx} \Delta\Theta(z; t-x)\,dx = 0\end{aligned}\right\} \tag{15}$$

with the boundary condition

$$\Delta\Theta(0; t) = 0 \tag{16}$$

that is inlet coolant temperature constant.

The solution of (15) is of the type

$$\Delta\Theta = \Delta\Theta(0; t) + \sum_{m=1}^{m=\infty} \frac{1}{m!} \left(\frac{\partial^m \Delta\Theta}{\partial z^m}\right)_{z=0} \cdot z^m \tag{17}$$

where all the $(\partial^m\Delta\Theta/\partial z^m)_{z=0}$ are functions of the time.

If in (15) we put $z = 0$, we get:

$$\left(\frac{\partial\Delta\Theta}{\partial z}\right)_{z=0} = 0. \tag{18}$$

Differentiating (15) in respect to "z" and putting $z = 0$, we get [taking into account (18)]:

$$\left(\frac{\partial^2\Delta\Theta}{\partial z^2}\right)_{z=0} = 0. \tag{19}$$

By successive differentiations we get for each "m"

$$\left(\frac{\partial^m\Delta\Theta}{\partial z^m}\right)_{z=0} = 0. \tag{20}$$

We can conclude that the solution of eq. (15) with the boundary condition (16) is:

$$\Delta\Theta(z;t)=0. \tag{21}$$

Acknowledgements

The author wishes to thank Prof. HÄFELE for the encouragement and for the useful discussions during the development of this work.

The author thanks also Miss FERRANTI who carried out the necessary calculations on the IBM 7070 computer.

References: [1] HÄFELE, W., K. OTT, L. CALDAROLA, SCHIKARSKI, COHEN, WOLFE, GREEBLER, and REYNOLDS: Static and Dynamic Measurements on the Doppler Effect in an Experimental Power Reactor. Geneva Conference 1964, A/CONF. 28/P/644. — [2] CALDAROLA, L., and SCHLECHTENDAHL: Reactor Temperature Transients with Spatial Variables — First Part: Radial Analysis. KFK 223, May 1964. — [3] COHEN, GREEBLER, HORST, and WOLFE: The Southwest Experimental Fast Oxide Reactor. GE-APED-4281 (June 1963).

Address: L. CALDAROLA
Institut für Angewandte Reaktorphysik
Kernforschungszentrum Karlsruhe
75 Karlsruhe

Druck der Universitätsdruckerei H. Stürtz AG., Würzburg